Upper limits to near-field radiative heat transfer: generalizing the blackbody concept

Upper limits to near-field radiative heat transfer: generalizing the blackbody concept

Owen D. Miller, Alejandro W. Rodriguez, Steven G. Johnson

Owen D. Miller, Alejandro W. Rodriguez, Steven G. Johnson, "Upper limits to near-field radiative heat transfer: generalizing the blackbody concept," Proc. SPIE 9920, Active Photonic Materials VIII, 99200B (16 September 2016); doi: 10.1117/12.2240718

SPIE.

Event: SPIE Nanoscience + Engineering, 2016, San Diego, California, United States

Invited Paper

Upper limits to near-field radiative heat transfer: Generalizing the "blackbody" concept

Owen D. Miller[a,b], Alejandro W. Rodriguez[c], and Steven G. Johnson[d]

[a]Department of Applied Physics, Yale University, New Haven, CT
[b]Energy Sciences Institute, Yale West Campus, West Haven, CT
[c]Department of Electrical Engineering, Princeton University, Princeton, NJ
[d]Department of Mathematics, Massachusetts Institute of Technology, Cambridge, MA

ABSTRACT

For 75 years it has been known that radiative heat transfer can exceed far-field blackbody rates when two bodies are separated by less than a thermal wavelength. Yet an open question has remained: what is the maximum achievable radiative transfer rate? Here we describe basic energy-conservation principles that answer this question, yielding upper bounds that depend on the temperatures, material susceptibilities, and separation distance, but which encompass all geometries. The simple structures studied to date fall far short of the bounds, offering the possibility for significant future enhancement, with ramifications for experimental studies as well as thermophotovoltaic applications.

Keywords: Radiative heat transfer, blackbody, thermophotovoltaics

1. INTRODUCTION

As the separation distance between a hot body and a cold one decreases to the micron scale and below, the rate at which radiative energy flows from the high-temperature body to the low-temperature one can greatly exceed the ray-optical blackbody limit.[1–4] Through Maxwell's equations and general energy-conservation principles, we bound how large this radiative "heat transfer" rate can be, yielding near-field limits that depend only on the material susceptibilities $\chi(\omega)$ and the separation distance d of the two bodies. We show that simple dipole–dipole and dipole–plate geometrical configurations approach restricted versions of the bounds, but that common large-area structures fall far short of the general bounds. By contrast, we find that particle arrays interacting in an idealized Born approximation (i.e., neglecting multiple scattering) exhibit both enhancement factors, suggesting the possibility of orders-of-magnitude improvement beyond previous designs, potentially enabling new levels of thermophotovoltaic-device performance.

Two physical principles underlie the blackbody limit to *far-field* radiative energy exchange between macroscopic objects: reciprocity (i.e. Kirchhoff's Law), and photon conservation.[5] The limit is a statement that every photon incident upon the surface of a blackbody is absorbed, and therefore emitted upon thermal excitation. At wavelength and subwavelength scales, however, scatterers can "bend" and amplify waves such that the number of photons "incident" upon a surface is either infinite or ill-defined, enabling greater-than-blackbody energy-exchange rates but preventing a simple analogous bound.

We circumvent the difficulties in photon counting by instead applying reciprocity and energy-conservation principles to the volume polarization currents induced within each of the bodies. Thermal absorbers and emitters must be lossy (i.e. have permittivities with a positive non-zero imaginary part), but lossy structures cannot support arbitrarily large currents—otherwise the dissipation would eventually be greater than the energy supplied by the incident fields,[6] violating passivity. Thus the intuitive understanding of our bounds is that resonant amplification of the incident fields can occur at most proportional to $|\chi|^2/\operatorname{Im}\chi$ for a material with susceptibility χ, while the incident fields rapidly increase with smaller separations in the near field, yielding two enhancement factors relative to the far-field blackbody limit.

Further author information: (Send correspondence to O.D.M.)
O.D.M.: E-mail: owen.miller@yale.edu

Active Photonic Materials VIII, edited by Ganapathi S. Subramania, Stavroula Foteinopoulou, Proc. of SPIE Vol. 9920, 99200B · © 2016 SPIE · CCC code: 0277-786X/16/$18 · doi: 10.1117/12.2240718

First we develop energy-conservation principles that bound how large currents can be in a lossy material, based on the simple premise that in passive systems the scattered power must be greater than zero. We show that such a statement applies very generally, whereby the "incident" and "scattered" fields can be selected any number of ways and positivity must still hold. We then apply this principle to the problem of radiative heat transfer, with thermal sources inside one of the scattering bodies, to yield the general bounds that comprise our primary result. Finally we compare the performance of the bounds to known configurations, showing that in certain cases they can be reached but that for large-area devices there is significant room for improvement.

2. ENERGY-CONSERVATION PRINCIPLES

The *optical theorem* equates the total power scattered or absorbed by any body to the imaginary part of a "forward-scattering amplitude"—in other words, to the amplitude and phase of an object's shadow.[7] Although typically written in terms of the overlap between real or effective surface currents with incident fields,[8] extinction (the sum of absorption and scattering), $P_{\text{ext}} = P_{\text{abs}} + P_{\text{scat}}$, can also be written in terms of the overlap between an incident field $\mathbf{E}_{\text{inc}}$ with the currents $\mathbf{P}$ induced in within the scatterer[9,10]

$$P_{\text{ext}} = \frac{\omega}{2} \operatorname{Im} \int_V \overline{\mathbf{E}}_{\text{inc}} \cdot \mathbf{P}, \tag{1}$$

which is simply the statement that extinction is the work done by the incident field on the induced currents (it can also be derived through the divergence theorem applied to the sum of the absorbed-power and scattered-power fluxes through the surface). In conjunction with the extinction we only need one other well-known quantity—the absorbed power—which is the work done by the *total* fields on the induced currents, i.e.[8]

$$P_{\text{abs}} = \frac{\omega}{2} \operatorname{Im} \int_V \overline{\mathbf{E}} \cdot \mathbf{P}. \tag{2}$$

Eqs. (1,2) already provide enough information to bound the magnitudes of the currents induced in any lossy scatterer, via the constraint that extinction be larger than absorption,

$$P_{\text{ext}} > P_{\text{abs}}, \tag{3}$$

or, equivalently, $P_{\text{scat}} > 0$. The crucial insight is that the extinction, per Eq. (1), is the imaginary part of a *linear* functional with respect to the induced currents $\mathbf{P}$, whereas absorption is a *positive definite quadratic* functional of the induced currents (since $\mathbf{E} = \frac{1}{\varepsilon_0 \chi}\mathbf{P}$). The constraint that absorption, a quadratic quantity, must be smaller than extinction, a linear quantity, imposes a limit to how large the currents can be before dissipation overtakes extinction, corresponding to unphysical negative scattered power. By variational calculus, the energy-conservation constraint given by Eq. (3) yields optimal currents $\mathbf{P}_{\text{opt}}$ proportional to

$$\mathbf{P}_{\text{opt}} \sim \frac{|\chi|^2}{\operatorname{Im} \chi} \mathbf{E}_{\text{inc}}, \tag{4}$$

with slightly different prefactors set by whether the figure of merit is absorption, scattered power, or extinction.

The passivity condition, $P_{\text{abs}} > P_{\text{scat}}$, is obvious for an isolated scatterer in free space, where it can be derived via imposition of outgoing radiation boundary conditions. Yet the condition applies for more general definitions of "incident" and "scattered" fields, a subtle extension that turns out to be crucial for the near-field radiative heat transfer bounds that we derive in Sec. 2.2.

2.1 Positivity of absorbed and scattered power

An interesting extension of the passivity condition in Eq. (3) is to the case when the incident field is defined not as a wave in a homogeneous medium (e.g. vacuum) but instead as the total field in the presence of a background scatterer. One can imagine, for example, a plane wave irradiating two objects that are close in proximity. If the figure of merit is the absorption or scattering of only *one* of the two objects, the "incident" field can be chosen as the total field when the plane wave scatters from the neighboring object, in which case the "scattered" field

arises only from the introduction of the second body into the problem (and $P_{\text{scat}} = 0$ without the second body). Here we show that $P_{\text{scat}} > 0$ in this general scenario, even though we cannot directly appeal to the radiation boundary conditions, since there is a body between the scatterer and the radiation "boundary" at infinity.

For simplicity we assume that our scattering problem can be accurately described by perfectly matched layers (PMLs) at some faraway distance, such that the scattering problem takes place in a finite volume consisting of the scatterer V and the exterior volume V^{ext}, joined by the surface S. This assumption is not required (one can use a more complicated combination of the steps below and then use of the radiation conditions), but it perhaps leads to more insight. With this partitioning of space, one can write the scattered power, which is the surface integral of the outward scattered-field Poynting flux, as the integral over the *exterior* volume by the divergence theorem:

$$\begin{aligned} P_{\text{scat}} &= \frac{1}{2}\operatorname{Re}\int_S \mathbf{E}_{\text{scat}} \times \overline{\mathbf{H}}_{\text{scat}} \cdot \hat{\mathbf{n}}, \\ &= -\frac{1}{2}\operatorname{Re}\int_{V^{\text{ext}}} \nabla \cdot \mathbf{E}_{\text{scat}} \times \overline{\mathbf{H}}_{\text{scat}} \\ &= \frac{\omega}{2}\operatorname{Im}\int_{V^{\text{ext}}} \left(\Delta\mu \left|\mathbf{H}_{\text{scat}}\right|^2 + \Delta\varepsilon \left|\mathbf{E}_{\text{scat}}\right|^2\right) > 0 \end{aligned} \tag{5}$$

where $\hat{\mathbf{n}}$ is the outward-pointing normal vector, and the third line followed from Maxwell's equations for the scattered fields, $\nabla \times \mathbf{E}_{\text{scat}} = i\omega\Delta\mu\mathbf{H}_{\text{scat}}$ and $\nabla \times \mathbf{H}_{\text{scat}} = -i\omega\Delta\varepsilon\mathbf{E}_{\text{scat}}$. Eq. (5) shows that the scattered power is given by the energy dissipated in the scattered field in the volume *external* to the scatterer, which must be greater than zero by the passivity conditions (Ref. 11) $\omega \operatorname{Im}\Delta\varepsilon > 0$ and $\omega \operatorname{Im}\Delta\mu > 0$. Even if the background scatterers are lossless, power is absorbed in the PMLs, and this absorption must also be positive.

Eq. (5) is a powerful general statement of the passivity condition $P_{\text{scat}} > 0$, and it enables a reciprocity-based approach to bound near-field thermal radiation.

2.2 Bounds on near-field radiative energy exchange

Radiative heat exchange is depicted schematically in Fig. 1(a): fluctuating currents arise in body 1 at temperature T_1, and transfer energy to body 2 at a rate of[4]

$$H_{1\to 2} = \int_0^\infty \Phi(\omega)\left[\Theta(\omega, T_1) - \Theta(\omega, T_2)\right] \mathrm{d}\omega, \tag{6}$$

where $\Phi(\omega)$ is a temperature-independent energy flux and Θ is the Planck spectrum. $\Phi(\omega)$ is the designable quantity of interest, to be tailored as a function of frequency depending on the application and available materials. The spectral heat flux $\Phi(\omega)$ is the power absorbed in body 2 from fluctuating sources in body 1 (or vice versa). We will use the generalized passivity condition derived above to derive a bound, even with thermal sources embedded *within* one of the scatterers.

We use a two-step process to understand the limits to the power transferred from body 1 to body 2. First, we reframe the scattering problem (without approximation), defining the "incident" field to be the unknown field emanating from body 1, and the "scattered" field to arise only with the introduction of body 2. For a Green's function (GF) $\boldsymbol{G}^1$ that is the field of dipole in the presence of body 1, the fields are given by a standard integral-equation separation,[12] $\mathbf{E}_{\text{inc},1} = (i/\varepsilon_0\omega)\int_{V_1} \boldsymbol{G}_1\mathbf{J}$ and $\mathbf{E}_{\text{scat},1} = \int_{V_2} \boldsymbol{G}_1\mathbf{P}$, where $\mathbf{J}$ are the stochastic source currents in body 1, $\mathbf{P}$ is the polarization field induced in body 2, and ε_0 is the vacuum permittivity. This decomposition permits an optimal theorem with respect to body 2, such that its extinction is proportional to $\operatorname{Im}\int_{V_2} \overline{\mathbf{E}}_{\text{inc},1} \cdot \mathbf{P}$. The positivity argument from above implies that absorption in body 2 is bounded,

$$P_{\text{abs},2} \le \frac{\varepsilon_0\omega}{2}\frac{|\chi_2(\omega)|^2}{\operatorname{Im}\chi_2(\omega)}\int_{V_2} |\mathbf{E}_{\text{inc},1}(\mathbf{x}_2)|^2, \tag{7}$$

which is formally derived by variational calculus.[6,13] To achieve this limit, the optimal polarization field must be proportional to the incident field, $\mathbf{P} \sim \mathbf{E}_{\text{inc},1}$, to maximize the extinction overlap integral. In the near field,

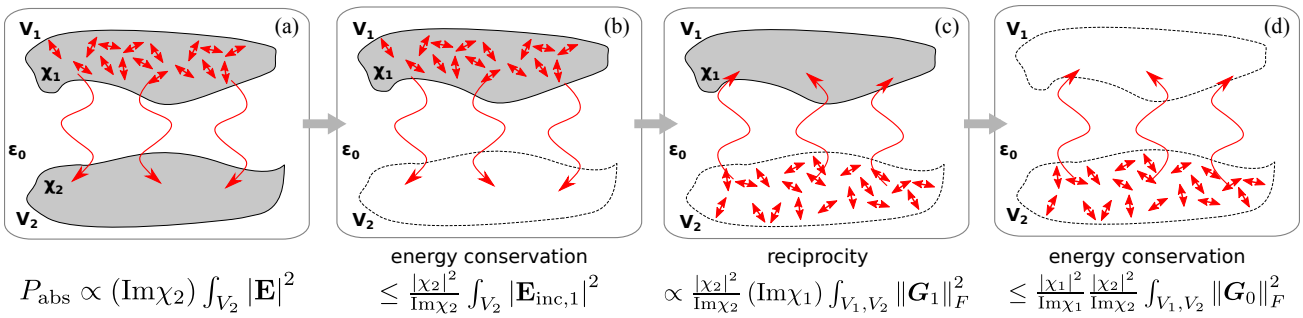

Figure 1. (a) Radiative heat transfer: Fluctuating currents in an emitter (body 1, susceptibility χ_1) generate a field $\mathbf{E}_{\rm inc,1}$ and transfer energy to an absorber (body 2, susceptibility χ_2) at a rate $P_{\rm abs,2}$. (b) Energy conservation bounds $P_{\rm abs,2}$ in terms of $\mathbf{E}_{\rm inc,1}$, and a resonant enhancement factor $|\chi_2|^2/\operatorname{Im}\chi_2$. (c) The sources and "receivers" can be exchanged by reciprocity, whereupon (d) absorption in body 1 is bounded, yielding a spectral-flux limit determined by χ_1, χ_2, and the free-space GF $\boldsymbol{G}_0$. For near-field transfer the GF integral is $\sim 1/d^2$, for separation d.

where source fields rapidly decay, negative-permittivity metals that support surface-plasmon modes can achieve this condition.

The limit in Eq. (7) reduces the optimal-flux problem to a question of how large the emitted field $\mathbf{E}_{\rm inc,1}$ can be in V_2. Inserting $\mathbf{E}_{\rm inc,1}$ into Eq. (7) yields an integral of the stochastic currents, which is determined by the fluctuation-dissipation theorem,[4] $\left\langle J_j(\mathbf{x},\omega), \overline{J_k(\mathbf{x}',\omega)} \right\rangle = 4\varepsilon_0\omega\Theta(\omega,T_1)\operatorname{Im}[\chi(\omega)]\,\delta_{jk}\delta(\mathbf{x}-\mathbf{x}')/\pi$. By reciprocity[14] one can exchange the positions in the integrand, $\mathbf{x}_1 \leftrightarrow \mathbf{x}_2$, such that emission from V_1 is equivalent to *absorption* for free-space sources in V_2, as in Fig. 1(c). Absorption is bounded by our energy conservation principle, limiting the emitted-field magnitude to

$$\left\langle |\mathbf{E}_{\rm inc,1}(\mathbf{x}_2)|^2 \right\rangle \leq 4\varepsilon_0\omega\Theta \frac{|\chi_1|^2}{\operatorname{Im}\chi_1} \int_{V_1} \|\boldsymbol{G}_0(\mathbf{x}_1,\mathbf{x}_2)\|_F^2 \,, \tag{8}$$

where $\boldsymbol{G}_0$ is the *free-space* GF, cf. Fig. 1(d). Inserting Eq. (8) into Eq. (7) and separating the Planck spectrum by Eq. (6), the maximum flux between two bodies is

$$\Phi(\omega) \leq \frac{2}{\pi} \frac{|\chi_1(\omega)|^2}{\operatorname{Im}\chi_1(\omega)} \frac{|\chi_2(\omega)|^2}{\operatorname{Im}\chi_2(\omega)} \int_{V_1}\int_{V_2} \|\boldsymbol{G}_0(\mathbf{x}_1,\mathbf{x}_2)\|_F^2 \,. \tag{9}$$

The limit of Eq. (9) can be further simplified. In the near field, $\boldsymbol{G}_0$ is ideally dominated by the quasistatic term $\sim 1/r^3$, which is primarily responsible for the evanescent waves that enable greater-than-black-body heat-transfer rates.[4,15] Dropping higher-order terms (further discussed in Ref. 13), we bound Eq. (9) by integrating over the infinite half-spaces containing V_1 and V_2, assuming a separating plane between the two bodies. (If not, e.g. between two curved surfaces, only the coefficients change.) For bodies separated by a distance d, the integral over the (infinite) area A is given by $\int_{V_1,V_2} \|\boldsymbol{G}_0\|_F^2 = A/32\pi d^2$, yielding flux limits per area or relative to a black body with flux $\Phi_{\rm BB} = k^2A/4\pi^2$:[4]

$$\frac{\Phi(\omega)}{A} \leq \frac{1}{16\pi^2 d^2} \frac{|\chi_1(\omega)|^2}{\operatorname{Im}\chi_1(\omega)} \frac{|\chi_2(\omega)|^2}{\operatorname{Im}\chi_2(\omega)}. \tag{10}$$

$$\frac{\Phi(\omega)}{\Phi_{\rm BB}(\omega)} \leq \frac{1}{4(kd)^2} \frac{|\chi_1(\omega)|^2}{\operatorname{Im}\chi_1(\omega)} \frac{|\chi_2(\omega)|^2}{\operatorname{Im}\chi_2(\omega)}. \tag{11}$$

Eqs. (9–11) are fundamental limits to the near-field spectral heat flux between two bodies. They arise from basic limitations to the currents that can be excited in dissipative media, and their derivations further suggest physical characteristics of the optimal response in near-field heat transfer: an *optimal emitter* enhances and absorbs near-field waves from reciprocal external sources *in the absence of the absorber* whereas an optimal absorber enhances and absorbs near-field waves from the emitter, *in the presence of the emitter*. These principles

can be understood by working backwards through Fig. 1. The optimal-emitter condition identifies the largest field that can be generated in an exterior volume (V_2) by considering the reciprocal absorption problem, per Fig. 1(c). Reinserting the absorber, cf. Fig. 1(b), should not reflect the emitted field but rather enhance and absorb it. Because heat flux is symmetric with respect to absorber–emitter exchange, both bodies should satisfy each condition (induced currents proportional to source fields). Eq. (9) can be interpreted as sources throughout the emitter generating free-space dipolar fields $\boldsymbol{G}^0$ enhanced by $|\chi_1|^2 / \operatorname{Im}\chi_1$, which are further enhanced by $|\chi_2|^2 / \operatorname{Im}\chi_2$ and absorbed. The dipole–dipole interactions are bounded by their separation distance,[16,17] leading to simple shape-independent limits in Eqs. (9–11). Ideal structures that achieve these limits can have significantly greater heat transfer than black bodies, even if their spectral flux has a narrow bandwidth. Whereas the heat transfer between black bodies in the far field is $H/A = \sigma_{\mathrm{SB}} T^4$, where σ_{SB} is the Stefan–Boltzmann constant,[5] a straightforward calculation shows that ideal near-field heat exchange over a narrow bandwidth $\Delta\omega/\omega = \operatorname{Im}\chi/|\chi|$, typical of plasmonic systems,[18,19] can achieve per-area transfer rates of[13]

$$\frac{H}{A} \approx \sigma_{\mathrm{SB}} T^4 \frac{2}{7(kd)^2} \frac{|\chi|^3}{\operatorname{Im}\chi}, \tag{12}$$

exhibiting both distance and material enhancements relative to the Stefan–Boltzmann rate.

2.3 Known-structure comparisons

If one of the bodies is small enough for its response to be dipolar, the optimal-absorber and optimal-emitter conditions converge: the polarization currents induced in each structure by free-space dipoles in place of the opposite structure must be proportional to the incident fields. This condition is satisfied for two-dipole transfer, and the enhancement of the emitted and absorbed fields is possible via "plasmonic" resonances in metallic nanoparticles. For two identical particles with volumes V, tip-to-center-of-mass distances r, and tip-to-tip separation d, Eq. (9) limits the flux:

$$[\Phi(\omega)]_{\text{dipole–dipole}} \leq \frac{3}{4\pi^3} \frac{|\chi_1(\omega)|^2}{\operatorname{Im}\chi_1(\omega)} \frac{|\chi_2(\omega)|^2}{\operatorname{Im}\chi_2(\omega)} \frac{V^2}{(2r+d)^6}. \tag{13}$$

The radiative flux between quasistatic metal spheres is known analytically[4] and peaks at the limit given by Eq. (13).

Heat transfer between a dipole and an extended structure is limited by integrating over the half-space occupied by any extended structure, yielding a maximum flux

$$[\Phi(\omega)]_{\text{dipole-to-ext}} \leq \frac{1}{8\pi^2} \frac{|\chi_1(\omega)|^2}{\operatorname{Im}\chi_1(\omega)} \frac{|\chi_2(\omega)|^2}{\operatorname{Im}\chi_2(\omega)} \frac{V}{(r+d)^3}, \tag{14}$$

where $r + d$ is the distance between the extended structure and the particle's center. Heat flux between a sphere and a bulk metal, each supporting a plasmonic mode, can achieve half of the maximum flux[4,20] if the resonances align. This geometry falls short by a factor of two because planar surface plasmons exist only for TM polarization,[21] and thus the planar structure reflects near-field TE-polarized light emitted by the sphere. Neither structure exhibits the $1/d^2$ enhancement factor, which for dipolar coupling ($\sim 1/d^6$) requires interactions over two extended areas.

Fig. 2(a) compares flux rates for sphere–sphere (orange circles) and sphere–plate (blue circles) geometries, computed by the fluctuating-surface current method,[22–24] to the limits of Eqs. (13,14) (orange and blue dashed lines, resp.). The spheres are modeled by Drude susceptibilities[8] with plasma frequency ω_p and loss rate $\gamma = 0.1\omega_p$. The "plate" is simulated by a very large ellipsoid (volume $\approx 7000\times$ larger than the sphere) comprising a material with a modified plasma frequency, $\omega_{p,\mathrm{pl}} = \sqrt{2/3}\omega_p$, and a modified loss rate, $\gamma_{\mathrm{pl}} = 2\gamma/3$, to align the resonant frequencies of the sphere and plate without modifying the flux limit. In each case the separation distance $d = 0.1c/\omega_{\mathrm{res}}$ and the sphere radii are $r = d/5$. The computations support the analytical result that the dipolar limits can be approached to within at least a factor of two.

For extended structures that do not behave like single dipoles, the optimal-absorber constraint is more demanding in that the absorber should enhance the emitted field while accounting for interactions between the

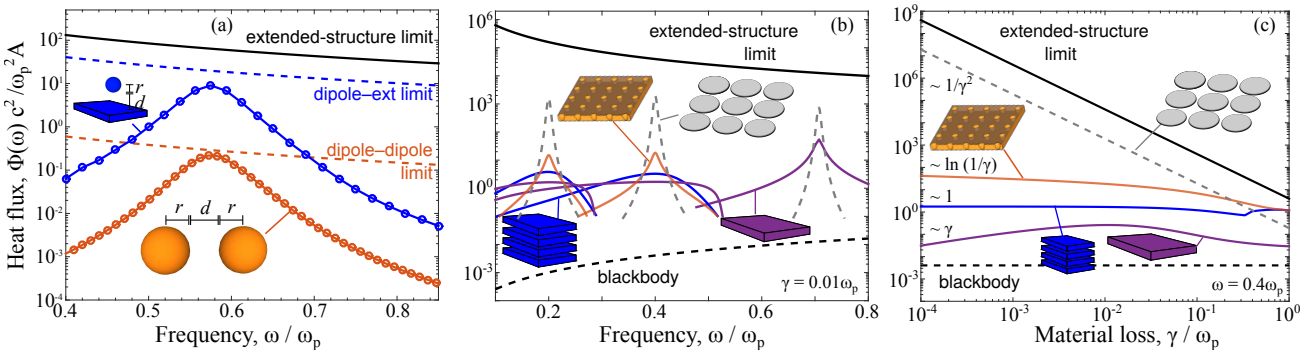

Figure 2. (a) Comparison of heat flux in sphere–sphere and sphere–plate structures to the analytical limits of Eqs. (13,14). Two Drude metal spheres (orange circles, fit to a solid line) approach the dipole–dipole limit (dashed orange) at their resonant frequency, $\omega_{\rm res} \approx \omega_p/\sqrt{3}$. A sphere and a plate (blue circles) approach within a factor of two of the limit between dipolar and extended objects (dashed blue). In each case the separation is $d = 0.1c/\omega_{\rm res}$, with sphere radii $r = d/5$. The flux rates exhibit the material enhancement factor $|\chi|^4/(\mathrm{Im}\,\chi)^2$, but not the near-field enhancement factor, due to the lack of large-area interactions. (b,c) Comparison of heat flux between mirror images of large-area Drude-metal structures separated by $d = 0.1c/\omega_p$. (b) Structures optimized for maximum flux at three frequencies, $\omega = (0.2, 0.4, 1/\sqrt{2})\omega_p$, for a material loss rate $\gamma = 0.01\omega_p$. Thin films (purple), hyperbolic metamaterials (blue), and elliptical metamaterials (orange) exceed black-body enhancements but fall far short of the limit (black) from Eq. (10). The dashed silver line represents the heat transfer for an idealized plasmonic-particle array without multiple scattering. (c) Optimized structures as a function of loss rate, for $\omega = 0.4\omega_p$. Each structure exhibits the $1/d^2$ near-field enhancement factor, but only the idealized particle array exhibits the $|\chi|^4/(\mathrm{Im}\,\chi)^2 \sim 1/\gamma^2$ material enhancement factor.

two bodies. We will show that common planar structures do not exhibit this behavior but that nanostructured media offer the possibility of approaching it.

Bulk metals (negative-permittivity materials) support surface plasmons that enable greater-than-blackbody heat flux at their resonant frequency. Individually, a single metal interface nearly satisfies the optimal-emitter condition, emitting near-field waves over a broad bandwidth of surface-parallel wavevectors (which enabled the nearly optimal sphere–plate transfer above). However, when a second metal is brought close to the first, it *reflects* most of the incident field, except over a narrow wavevector-bandwidth, due to multiple-scattering effects between the bodies. The failure of the two-metal geometry to achieve the optimal-absorber condition leads to a peak spectral heat flux, at the surface-plasmon frequency $\omega_{\rm sp}$, of approximately[13]

$$\left[\frac{\Phi(\omega_{\rm sp})}{A}\right]_{\text{plate-to-plate}} = \frac{1}{4\pi^2 d^2}\ln\left[\frac{|\chi|^4}{4(\mathrm{Im}\,\chi)^2}\right] \tag{15}$$

which is significantly smaller than the limit in Eq. (10) due to the weak, logarithmic material enhancement. The shortcomings of the bulk-metal interactions cannot be overcome with simple metamaterial or thin-film geometries. The flux rate between hyperbolic metamaterials (HMMs) is material-independent.[25] Optimal thin films behave similarly to HMMs,[26] thereby also falling short of the limits. "Elliptical" metamaterials, with nearly isotropic effective permittivities, exhibit resonances for $\chi_{\rm eff} \approx -2$ and thus transfer heat at a rate similar to Eq. (15), limited by the same interference effects discussed above, and because $|\chi_{\rm eff}|^4 \ll |\chi|^4$.

Fig. 2(b,c) demonstrates the shortcomings of such structures, showing the computed heat flux between mirror images of thin-film (purple), hyperbolic-metamaterial (blue), and elliptical-metamaterial (orange) structures, as a function of (b) frequency and (c) material-loss rate, for a fixed separation $d = 0.1c/\omega_p$. The structural parameters are computationally optimized using a derivative-free local optimization algorithm.[27,28] Fig. 2(c) shows that the sub-optimal performance can be attributed primarily to the fact that the structures do not exhibit the material enhancement factor $|\chi|^4/(\mathrm{Im}\,\chi)^2 \sim 1/\gamma^2$, as predicted by Eq. (15) and due to the significant reflections in such geometries.

The spectral heat flux of the limit in Eq. (9) can be interpreted as the exchange of enhanced free-space dipole fields, as discussed above. Guided by this intuition, we include in Fig. 2(b,c) the heat flux between

close-packed arrays of oblate disk ellipsoids (dashed silver lines), small enough to be dipolar. We idealize their response as the additive sum of Eq. (13) over a lattice neglecting multiple scattering (i.e. in a Born approximation)[29] and accounting for the polarization-dependence of non-spherical ellipsoids.[30] This structure combines the individual-particle interactions that exhibit the material enhancement (which planar bodies do not) with the large-area interactions that exhibit $1/d^2$ near-field enhancement (which isolated bodies do not). Fig. 2(b,c) suggests the possibility for two to three orders of magnitude enhancement by periodic structuring and tailored local interactions.

ACKNOWLEDGMENTS

ODM and SGJ were supported by the Army Research Office through the Institute for Soldier Nanotechnologies under Contract No. W911NF-07-D0004, and by the AFOSR Multidisciplinary Research Program of the University Research Initiative (MURI) for Complex and Robust On-chip Nanophotonics under Grant No. FA9550-09-1-0704. AWR was supported by the National Science Foundation under Grant No. DMR-1454836.

REFERENCES

[1] Polder, D. and Van Hove, M., "Theory of Radiative Heat Transfer between Closely Spaced Bodies," *Phys. Rev. B* **4**(10), 3303–3314 (1971).

[2] Rytov, S. M., Kravtsov, Y. A., and Tatarskii, V. I., [*Principles of Statistical Radiophysics*], Springer-Verlag, New York, NY (1988).

[3] Mulet, J.-P., Joulain, K., Carminati, R., and Greffet, J.-J., "Enhanced Radiative Heat Transfer at Nanometric Distances," *Microscale Thermophys. Eng.* **6**(3), 209–222 (2002).

[4] Joulain, K., Mulet, J.-P., Marquier, F., Carminati, R., and Greffet, J.-J., "Surface electromagnetic waves thermally excited: Radiative heat transfer, coherence properties and Casimir forces revisited in the near field," *Surf. Sci. Rep.* **57**, 59–112 (2005).

[5] Lienhard IV, J. H. and Lienhard V, J. H., [*A Heat Transfer Textbook*], Dover, 4th ed. (2011).

[6] Miller, O. D., Polimeridis, A. G., Homer Reid, M. T., Hsu, C. W., DeLacy, B. G., Joannopoulos, J. D., Soljačić, M., and Johnson, S. G., "Fundamental limits to optical response in absorptive systems," *Opt. Express* **24**(4), 3329–64 (2016).

[7] Newton, R. G., "Optical theorem and beyond," *Am. J. Phys.* **44**(7), 639–642 (1976).

[8] Jackson, J. D., [*Classical Electrodynamics, 3rd Ed.*], John Wiley & Sons (1999).

[9] Lytle, D. R., Carney, P. S., Schotland, J. C., and Wolf, E., "Generalized optical theorem for reflection, transmission, and extinction of power for electromagnetic fields," *Phys. Rev. E* **71**, 056610 (2005).

[10] Hashemi, H., Qiu, C.-W., McCauley, A. P., Joannopoulos, J. D., and Johnson, S. G., "Diameter-bandwidth product limitation of isolated-object cloaking," *Phys. Rev. A* **86**, 013804 (2012).

[11] Welters, A., Avniel, Y., and Johnson, S. G., "Speed-of-light limitations in passive linear media," *Phys. Rev. A* **90**, 023847 (2014).

[12] Chew, W. C., [*Waves and Fields in Inhomogeneous Media*], IEEE Press (1995).

[13] Miller, O. D., Johnson, S. G., and Rodriguez, A. W., "Shape-Independent Limits to Near-Field Radiative Heat Transfer," *Phys. Rev. Lett.* **115**, 204302 (2015).

[14] Rothwell, E. J. and Cloud, M. J., [*Electromagnetics*], CRC Press (2001).

[15] Basu, S., Zhang, Z. M., and Fu, C. J., "Review of near-field thermal radiation and its application to energy conversion," *Int. J. Energy Res.* **33**, 1203–1232 (2009).

[16] Piestun, R. and Miller, D. A. B., "Electromagnetic degrees of freedom of an optical system," *J. Opt. Soc. Am. A* **17**(5), 892 (2000).

[17] Miller, D. A. B., "Communicating with waves between volumes: evaluating orthogonal spatial channels and limits on coupling strengths.," *Appl. Opt.* **39**(11), 1681–1699 (2000).

[18] Wang, F. and Shen, Y. R., "General Properties of Local Plasmons in Metal Nanostructures," *Phys. Rev. Lett.* **97**, 206806 (2006).

[19] Raman, A., Shin, W., and Fan, S., "Upper Bound on the Modal Material Loss Rate in Plasmonic and Metamaterial Systems," *Phys. Rev. Lett.* **110**, 183901 (2013).

[20] Mulet, J. P., Joulain, K., Carminati, R., and Greffet, J. J., "Nanoscale radiative heat transfer between a small particle and a plane surface," *Appl. Phys. Lett.* **78**(19), 2931–2933 (2001).
[21] Maier, S. A., [*Plasmonics: Fundamentals and Applications*], Springer Science & Business Media (2007).
[22] Reid, M. T. H., "scuff-EM: Free, open-source boundary-element software," *http://homerreid.com/scuff-EM* .
[23] Rodriguez, A. W., Reid, M. T. H., and Johnson, S. G., "Fluctuating-surface-current formulation of radiative heat transfer for arbitrary geometries," *Phys. Rev. B* **86**(22), 220302 (2012).
[24] Rodriguez, A. W., Reid, M. T. H., and Johnson, S. G., "Fluctuating-surface-current formulation of radiative heat transfer: Theory and applications," *Phys. Rev. B* **88**, 54305 (2013).
[25] Biehs, S.-A., Tschikin, M., and Ben-Abdallah, P., "Hyperbolic Metamaterials as an Analog of a Blackbody in the Near Field," *Phys. Rev. Lett.* **109**, 104301 (2012).
[26] Miller, O. D., Johnson, S. G., and Rodriguez, A. W., "Effectiveness of Thin Films in Lieu of Hyperbolic Metamaterials in the Near Field," *Phys. Rev. Lett.* **112**, 157402 (2014).
[27] Powell, M. J. D., "A direct search optimization method that models the objective and constraint functions by linear interpolation," in [*Advances in Optimization and Numerical Analysis*], 51–67, Springer (1994).
[28] Johnson, S. G., "The NLopt nonlinear-optimization package," *http://ab-initio.mit.edu/nlopt* .
[29] Phan, A. D., Phan, T.-L., and Woods, L. M., "Near-field heat transfer between gold nanoparticle arrays," *J. Appl. Phys.* **114**(21), 214306 (2013).
[30] Bohren, C. F. and Huffman, D. R., [*Absorption and Scattering of Light by Small Particles*], John Wiley & Sons, New York, NY (1983).